Vol. 15, No. 2 (2016) 469-480
Revista Mexicana de Ingeniería Química

MORPHO-STRUCTURAL DESCRIPTION OF UNRIPE AND RIPE AVOCADO PERICARP (*Persea americana* Mill VAR. DRYMIFOLIA) DESCRIPCIÓN MORFO-ESTRUCTURAL DEL PERICARPIO DEL AGUACATE (*Persea americana* Mill VAR. DRYMIFOLIA) INMADURO Y MADURO

R. Espinosa-Velázquez[1], L. Dorantes-Alvarez[1]*, G.F. Gutiérrez-López[1], E. García-Armenta[2], L. Sánchez-Segura[3], M.J. Perea-Flores[4], G.M. Ceballos-Reyes[5], A. Ortíz Moreno[6]

[1] *Departamento de Graduados en Alimentos, Escuela Nacional de Ciencias Biológicas, Instituto Politécnico Nacional. Ciudad de México, c.p. 07738, México.*

[2] *Doctorado en Ciencias, Especialidad Biotecnología (Programa Regional del Noroeste para el Doctorado en Biotecnología) FCQB-AS, Ciudad Universitaria, A.P. 1354, c.p. 80000, Culiacán, Sinaloa, México.*

[3] *Departamento de Ingeniería Genética, CINVESTAV, Instituto Politécnico Nacional, Unidad Irapuato Km 9.6 Libramiento Norte Carretera Irapuato-León c.p. 36821, Irapuato, Guanajuato, México.*

[4] *Centro de Nanociencias y Micro y Nanotecnologías, Instituto Politécnico Nacional. Luis Enrique Erro s/n, Col. Unidad Profesional Adolfo López Mateos, Ciudad de México, c.p. 07738, México.*

[5] *Unidad de Investigación Cardiometabólica, Escuela Superior de Medicina, Instituto Politécnico Nacional, Ciudad de México, Del. Miguel Hidalgo,c.p. 11340, México.*

[6] *Departamento de Biotecnología, Escuela Nacional de Ciencias Biológicas, Instituto Politécnico Nacional, Ciudad de México, c.p. 07738, México.*

Received May 31, 2016; Accepted June 6, 2016

Abstract

Digital Image Analysis (DIA) was applied to pericarp tissues of unripe and ripe avocado var. drymifolia with the aim to describing morpho-structural features. When these tissues were observed under optical microscope, differences were found between both ripening stages: the unripe tissue had an exocarp with single epidermis cells in vertical disposition and a mesocarp with a dispersed monolayer of isodiametrical cells; the ripe tissue showed thickened cell walls with sclerenchymal tissue formation. Parenchymal tissue presented homogeneous shape and a bigger cell size. The Confocal Laser Scanning Microscopy also showed differences between the two ripening stages: unripe displayed two autofluorescence signals, corresponding to lignin and chlorophylls, while in ripe, a third signal was observed that corresponded to anthocyanins. The analysis of RGB channels analysis showed differences, with the ripe tissue demonstrating more intensity, reflecting pigments accumulation. Regarding the fractal analysis, Fractal dimension (F_D) resulted higher for ripe tissues due to the irregular arrangement of cells whereas, F_D and lacunarity (Λ) analysis per tissue section demonstrated a morphology change in the section where lipid cell accumulation occurs.

Keywords: avocado, pericarp, digital image analysis, microscopy, fractal dimension.

Resumen

Se realizó Análisis Digital de Imágenes en el tejido del pericarpio de aguacate variedad drymifolia inmaduro y maduro, con el objetivo de describir algunas características morfo-estructurales. Se observaron tejidos con el microscopio óptico, encontrando diferencias entre ambos tejidos: el tejido inmaduro mostró un exocarpo con una epidermis con monocapa en disposición vertical y un mesocarpo con una monocapa de células isodiamétricas; el tejido maduro mostró un engrosamiento en las paredes celulares, con formación de esclerénquima y una importante concentración de antocianinas, el tejido parenquimal presentó una forma más homogénea y un mayor tamaño celular. La microscopía confocal de barrido láser también mostró diferencias entre ambos tejidos: el inmaduro emitió dos señales de autofluorescencia, que correspondieron a lignina y clorofilas, mientras que el maduro, emitió una tercera señal, correspondiente a antocianinas. El análisis RGB también mostró diferencias, con mayor intensidad en el maduro, reflejando una acumulación de pigmentos. Con respecto al análisis fractal, la Dimensión fractal (D_F) resultó mayor en el tejido inmaduro, debido a una distribución celular irregular, mientras que en el análisis por sección de tejido la D_F y lagunaridad (Λ) demostraron un cambio de morfología en la sección de tejido donde ocurre la acumulación de lípidos.

Palabras clave: aguacate, pericarpio, análisis digital de imágenes, microscopia, dimensión fractal.

* *Corresponding author. E-mail*: ldoran@ipn.mx
Tel 57296000 ext57868

1 Introduction

Avocado fruit is a berry of one carpel containing a single seed. During early stages of growth, the pericarp is composed of three tissues: the exocarp or skin, the mesocarp or fleshy portion, and the endocarp, which is the thin inner layer that covers the seed (Cummings and Schroeder, 1942). However, the description of the tissue organization of avocado variety drymifolia is different to the more commercial varieties and has, as main feature, that its exocarp or peel is smooth and thin, with colour variation between dark green and black (Domínguez *et al*., 2014). Avocado (*Persea americana* Mill) var. drymifolia is an endemic fruit from Mexico with a production reaching of 35155 tons in 2014 (SIAP) and studies about its composition are scarce (Acosta-Díaz E., 2012). However, its edible skin may constitute an important source of a number of bioactive compounds. There are studies that report the presence of different bioactive compound groups in the exocarp of other avocado varieties as in Hass, Fuerte and Choquette, such as pigments and phenolic compounds. (Wang *et al*., 2010, Kosinska *et al*., 2011). Pigments as anthocyanins, have received increased attention due to their high antioxidant potential (Cerón-Montes, G.I. *et al*., 2015), and their stimulating health benefits such as improving visual acuity through rodopsin generation (Lila, 2004), decreasing cancer tumor growth, and to inhibit bacterial cell adhesion in the urinary tract (Fang-Chiang and Wrolstad, 2005). Others, as for example, chlorophylls, have also demonstrated to promote different biological activities:antioxidant, antimutagenic, and apoptosis induction in cancer cell lines (Delgado-Pelayo *et al*., 2014).Furthermore, the drymifolia exocarp ingestion would also help to meet dietary fiber requirements.

The anatomy of the avocado fruit is different among varieties and ripening stages, (Schroeder, 1953). In general, ripe avocado exocarp has been described as having epidermis, parenchymal, subepidermal cell layers and an irregular zone with sclerenchymal cells (Fisher, 1989). The increase in the cell wall thickness, and, therefore, the fruit size, results from cell expansion and division. In avocado, the cells under the epidermis are small and elongated and at about1.5 mm beneath those, the parenchymal cells can be found, with a bigger size and with rounded or isodiametric shapes with sizes that remain constant in the rest of the pericarp, except in the vascular union region. (Schroeder, 1953). The edible part, the mesocarp, is composed of parenchymal cells and some specialized ones, such as the idioblasts, that are lipid-storage cells (Donetti, 2011).

A study on the structure and morphology of the avocado fruit carried out by Cummings and Schroeder (1950) showed differences between thick-skinned and thin-skinned avocado types which resulted from the amount and density of stone-cell masses located beneath the epidermis. Varieties with thick skin, such as Hass avocado, have a layer of densely packed sclerenchyma while thin-skinned varieties like Drymifolia contain only small scattered groups of sclerenchyma. There have been a number of comprehensive studies concerning fruit ripening physiology in which Hass and other commercial varieties avocados are mentioned (Rhodes, 1981).

The growth and maturation of fruits have received scientific scrutiny because of the uniqueness of such processes and the importance of this fruit as a significant component of the human diet (Giovanonni, 2011). Avocado follows a similar trend to other fruits, with rapid cell division at the early stages of maturation; multiplication continues in the mature fruit while avocado is still attached to the tree and do not ripe until harvested (Seymor and Tucker,1993). There are also changes of colour in skin avocado, from green to purple/black as the fruit ripens (and observed as a decrease in L, chroma and hue angle) (Cox, K.A., 2003).

Novel tools such as Digital Image Analysis (DIA), have been used to obtain information from physical changes in maturation in different fruits, including banana (Quevedo *et al*., 2008) and avocado (whole fruit and skin) Hass (Arzate-Vázquez *et al*., 2011); but there are no reports of the use of DIA for the evaluation of avocado var. drymifolia pericarp tissues.

DIA has been defined as the construction of explicit, meaningful and quantitative descriptions of objects from obtained images (Kodagali and Balaji, 2012). The information obtained from digital images can be processed since these can be interpreted by numeric algorithms contained in specific software (Aguilera, 2001).

Fractal dimension (F_D) is a measure of irregularity and is based on the self-similarity of objects (Mandelbrot, 1983). In food science, the fractal dimension has been a useful parameter to evaluate changes in physical and chemical properties (Santacruz-Vázquez C. *et al*., 2007). Lacunarity (Λ), on the other hand, is a measure of the amount and distribution of spaces or gaps in a certain image that are not filled totally or partially by the analyzed object (Kilic and Abiyev, 2011), and

was originally developed to distinguishing among fractal objects having the same fractal dimension (Mandelbrot, 1983); is a relatively new feature to describe morphology of objects (Borys *et al*., 2008).

Another texture characteristic that can be obtained through DIA is the image entropy that is a measurement of the randomness of an image (Fernández L. *et al*, 2005).

Thus, the use of fractal dimension, lacunarity and entropy, represents a rather novel approach to provide a more complete description of microstructure related features.

Color is considered a fundamental physical property of foods that can be analyzed by DIA (Mendoza *et al*., 2006). The RGB model is an additive color model that uses transmitted light to display colors, thus, colored pixels are produced by firing red, green and blue and the color relates closely to the way human perceives it in the retina (Yam and Papdakis, 2004). This color model is the most used and allows detecting small color characteristics of the object and to carry out a global analysis of it as a color histogram (León K., *et al*., 2006).

Another tool that allows examining the internal structure of biological tissues is the Confocal Laser Scanning Microscopy. This technique produces optical sections through a three-dimensional specimen, (Durrenberger M.B., *et al*., 2001) giving the possibility to analyze structures and composition of a given sample and is able to capture fluorescent tissue specimens in detail (Paddock, S.W., 1999). Also, and fluorescent specific compounds can be detected through specific excitation/emission wavelengths.

The aim of this work was to perform a digital image analysis to describe the morphological characteristics and the distribution of some compounds in the pericarp tissue of unripe and ripe avocado var. drymifolia.

2 Materials and methods

2.1 Materials

Avocados (*Persea americana* Mill var. drymifolia) from a single batch, were cropped in Ocuituco, Morelos, México (Latitude: 18°52'3" N, Longitude 98°46'31" W, Altitude 1933 m above sea level). Avocados had a post anthesis period of 5 months and were designated as unripe when they presented aproximately 80 % moisture and an exocarp with a green color, and were designated as ripe when they reached aproximately 65% moisture and an exocarp with dark purple color.

2.2 Optical microscopy

Transversal histological sections,10 μm width from avocado tissue var. drymifolia unripe and ripe, previously mounted with a Tissue Freezing Medium (Leica, Germany) were obtained with a sliding freezing microtome CM 1850 (Leica, Germany), and observed under the optical microscope ElipseTi-U (Nikon, Japan) at 20x, 40x and 60x. Halogen lamp was used for lightening as transmitted light.

2.3 Digital Image Analysis (DIA)

Colour images of the avocado peel tissue were analysed by using the ImageJ v.1.49p software (National Institutes of Health, Bethesda, USA) to obtain histogram plots of each RGB (Red, Green and Blue) channels.

Global fractal dimension (F_D) and lacunarity (Λ) were evaluated by using the same software and converting the original image (RGB) to an 8-bits format (grey scale). An automatic threshold was carried out for segmentation and to get binary image. Finally, the images were uploaded in batch in the plugin Frac-Lac (2015Febb5810).

In order to evaluate morphology along the tissue, sections of monolayer cells, having an average size of 219 x 26 pixels at scale: 1.21 pixels/μm were cropped from the original image, resulting in 13 sections (Fig.1). Field of view (FOV) of each crop was 3900 μm^2. Λ and F_D and image entropy were evaluated for each section.). F_D an Λ were calculated using the box-counting method, thus, evaluating the number of grid boxes that touches the image (Nr) by using square grids of descending size (r) and digitally superimposed to the object, F_D is calculated as the slope of the straight line (Eq. 1) (Sánchez-Segura *et al*. 2015):

$$F_D = \log N_r vs. \log\left(\frac{1}{r}\right) \tag{1}$$

Lacunarity was calculated from the standard deviation (σ) and the mean (η) for pixels per box at the selected size (r), in a box count (g) (Eq. 2) (García-Armenta E. *et al*., 2016):

$$Lacunarity = \left(\frac{\sigma}{\eta}\right)^2_{r,g} \tag{2}$$

Entropy was calculated with the following equation (Eq. 3) (Fernández L. *et al.*, 2005):

$$Entropy = -\sum_i \sum_j p(i,j)\log\{p(i,j)\} \qquad (3)$$

Where $p(i, j)$ is the input to a dependence matrix of spatial gray levels.

2.4 *Confocal Laser Scanning Microscopy (CLSM)*

Several observations were made by means of confocal laser scanning microscope with the same avocado tissue sections used in optical microscopy. The Confocal Microscope used was a LSM 710 NLO, (Carl Zeiss, Jena, Germany). Tissue was excited with a laser scanning from 400 to 700 nm laser lines, and the emission autofluorescence spectrum was detected between 422 and 722 nm. These were compared against spectrum emission from commercial standards (Chlorophylls, Lignin, Cyanidine 3-O glucoside, all from Sigma-Aldrich, Germany) following the same procedure.

2.5 *Statistical analysis*

Analysis of variance (ANOVA) was performed for evaluating the significance of fractal dimension (F_D) and lacunarity (Λ). Correlation between F_D and Λ was evaluated with Pearson's coefficient. The significance of the analyses was 95% with p <0.05. The software used for this analysis was Minitab 16.0.

3 Results and discussion

3.1 *Unripe avocado*

The exocarp was composed of single epidermis cells in vertical disposition (Fig. 1A). This monolayer of cells was covered with a thick cuticle of a wax-like film on the surface of the fruit. Subsequently, a hypodermis composed of three layers of elongated cells was observed followed by a dispersed monolayer of isodiametrical, meristematic cells that formed the mesocarp (Fig. 1A). Meristematic cells are fundamentally similar to young parenchymal cells (Evert, 2006). Finally, parenchymal cells were observed, with isodiametrical form (Fig. 1A), which were larger than meristematic ones (Azcárraga-Rossette, *et al.*, 2010).

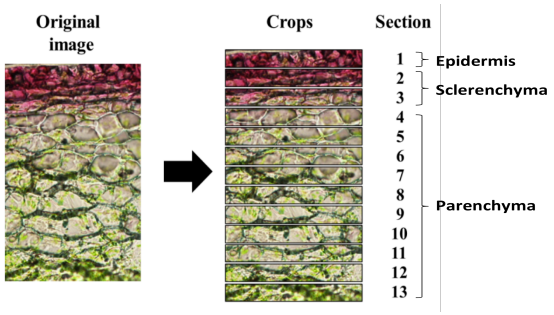

Figure 1. Schematic representation of the cropping method to obtain 13 sections of the avocado tissue image for performing digital image analysis.

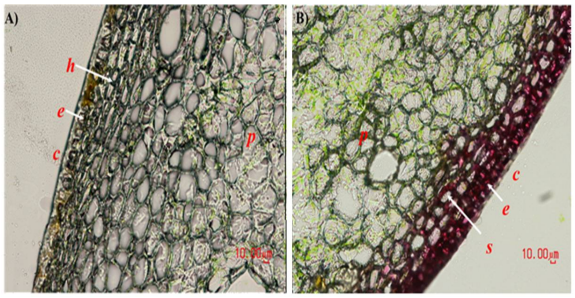

Figure 2. Tissular organization of fruit avocado var. drymifolia in different stages of growth view by optical microscopy. A) Unripe avocado, the thick cuticle (c) coats the epidermis (e) whilst, the hypodermis (h) limits the parenchyma (p) tissue. B) In ripe fruit, a thinner (as compared to unripe avocado) cuticle was observed (c) and epidermis cells showed lignified walls (e), the anthocyanin pigments were stored in the sclerenchyma tissue (s), and the parenchyma tissue (p) had cells with lipid accumulation (idioblasts).

The increase in size was due to the specialized of compartmentalization function, mainly of lipid storage (idioblasts) and chlorophyll (chloroplast) during development (Donetti, 2011).

3.2 *Ripe avocado*

The ripe fruit of avocado var. drymifolia, showed a composition of tissues similar to the unripe fruit. However, in the epidermis cells a decreased size, thickening of cell walls (lignified walls) and diminution of cuticle was observed in ripe avocado, probably due to the change in lipid composition that covers the fruit surface (Fig. 2B). The most important change was observed in the subsequent three cell layers that showed lignified thick walls, no elongation, expansion and cell division, indicating that a sclerenchyma tissue formation was carried out

(Fig. 2B). The sclerenchyma is the layer which is removed when the fruit is peeled in commercial stages and delimits the inner boundary in the maturing fruit (Fisher and Davenport, 1989), in addition, an increase in pigments accumulation in this tissue was observed (Fig. 2B). Subsequently, the prominent parenchymal tissue in the mesocarp (edible portion) was found and these cells showed homogenous shape and an increased content in lipids and tannins (Fig. 2B), the cell size was bigger in ripe fruits than in unripe-sate ones.

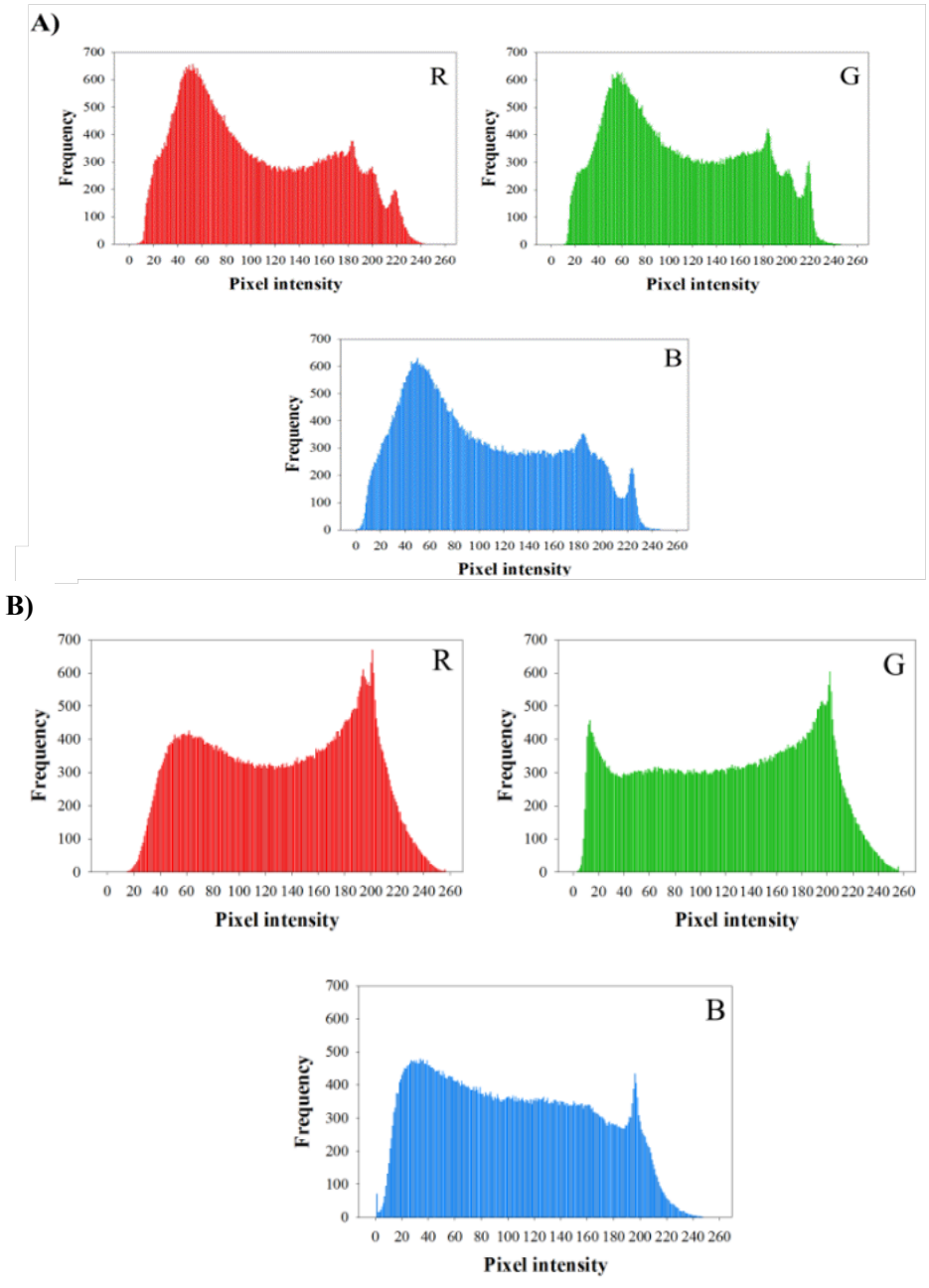

Figure 3. Histogram plots of RGB channels for A) Unripe avocado pericarp and B) Ripe avocado pericarp.

3.3 RGB channels analysis

Results showed that pixel intensities of RGB channels for unripe peel avocado had a lower value, which can explain darker color with less luminosity (Figure 3). A mode of the histogram plots for R, G and B channels was observed between 20 and 80. Few pixels were observed in higher values.

Brighter colors were observed for ripe peel avocado. The mode of the histogram plots for R, G and B channels was located towards higher values of pixel intensity (200). In the Blue channel the frequency was lower in comparison to Red and Green ones. When the red channels between unripe and ripe avocado tissues were compared, a significant difference was found ($p< 0.05$), with more intensity in the ripe tissue. This could be the result of anthocyanins accumulation in the exocarp. Anthocyanins have long been discussed to act as a screen against UV-B light and studies have proven that anthocyanins mask the chlorophyll containing organelles and thereby, protect chloroplasts against high light intensities to prevent photoinhibition (Stintzing F.C., Carle R., 2004).

The same result was observed in Green channels between unripe and ripe tissues, with a significant difference between them ($p<0.05$), and also more intensity in the ripe, probably due to a rise in chlorophylls concentration in the avocado tissues. The Blue channels did not show any differences ($p>0.05$) between unripe and ripe avocado.

3.4 Morphometric and texture parameters

In this work, texture fractal dimension (F_D) was a measure of the irregularity of the tissue (Mandelbrot, 1986), and the arrangement of the cells that were part of the peel (Table 1). A significant higher ($p < 0.05$) value of F_D was observed for the unripe tissue in comparison to the ripe tissue. Therefore, the unripe avocado presented amore irregular arrangement of cells, which were affected by the ripening stage.

On the other hand, the ripening stage influenced lacunarity values, which were significantly different ($p < 0.05$) among them. In average, lacunarity was higher for unripe peel avocado, which was related to a higher symmetry in the tissue. The lacunarity measures the distribution of the irregularity (determined by F_D) within the image (Mandelbrot, 1983). However, the variation of the results was higher and was reflected in the corresponding standard deviations of lacunarity values, which was a consequence of the heterogeneity of the tissue.

Values for the first four sections of tissue were higher than those for ripe fruit up to the intersection point (IP) where a change in tendency was observed *i.e.*, ripe tissue values where higher than those for the unripe one (Figure 5). However, for lacunarity, a contrary effect was observed (Figure 6); the first three sections presented higher values for the ripe tissue up to the intersection point where a charge in tendency was observed.

The IP was roughly located where the idioblasts start to appear. IP defines morphometry and symmetry changes of the unripe-ripe tissue. This point was obtained in F_D= 2.59 and Λ = 0.09 which falls in the straight line of Figure 7 so indicating a linear proportion between the filling of spaces and its irregularity.

Irregularity and heterogeneity of the avocado peel in different ripening stages was described by image entropy, which is a measure of the randomness of the pixel intensity within the image (Qiu-Ming, *et al.* 2007). Image entropy was significantly higher ($p < 0.05$) for ripe avocado peel, which indicated a less uniformity in pixel intensity with a higher irregularity in texture.

Figure 4 shows the surface plots for each ripening stage. Darker pixels were observed at the exocarp (top of the section: orientation towards 338 pixels) for both stages; the ripe surface plot darker zone is more pronounced due to the presence of cells with better arrangement and to the augmented anthocyanin concentration, both conditions also observed under optical microscope.

Table 1. Morphometric and texture parameters for each ripening stage of the avocado pericarp.

	AVOCADO PERICARP RIPENING STAGE	
Parameter	Unripe*	Ripe*
F_D	2.83 ± 0.01	2.80 ± 0.01
Λ	0.10 ± 0.05	0.02 ± 0.01
Entropy	9.18 ± 0.16	9.36 ± 0.15

*Mean and its corresponding standard deviation.

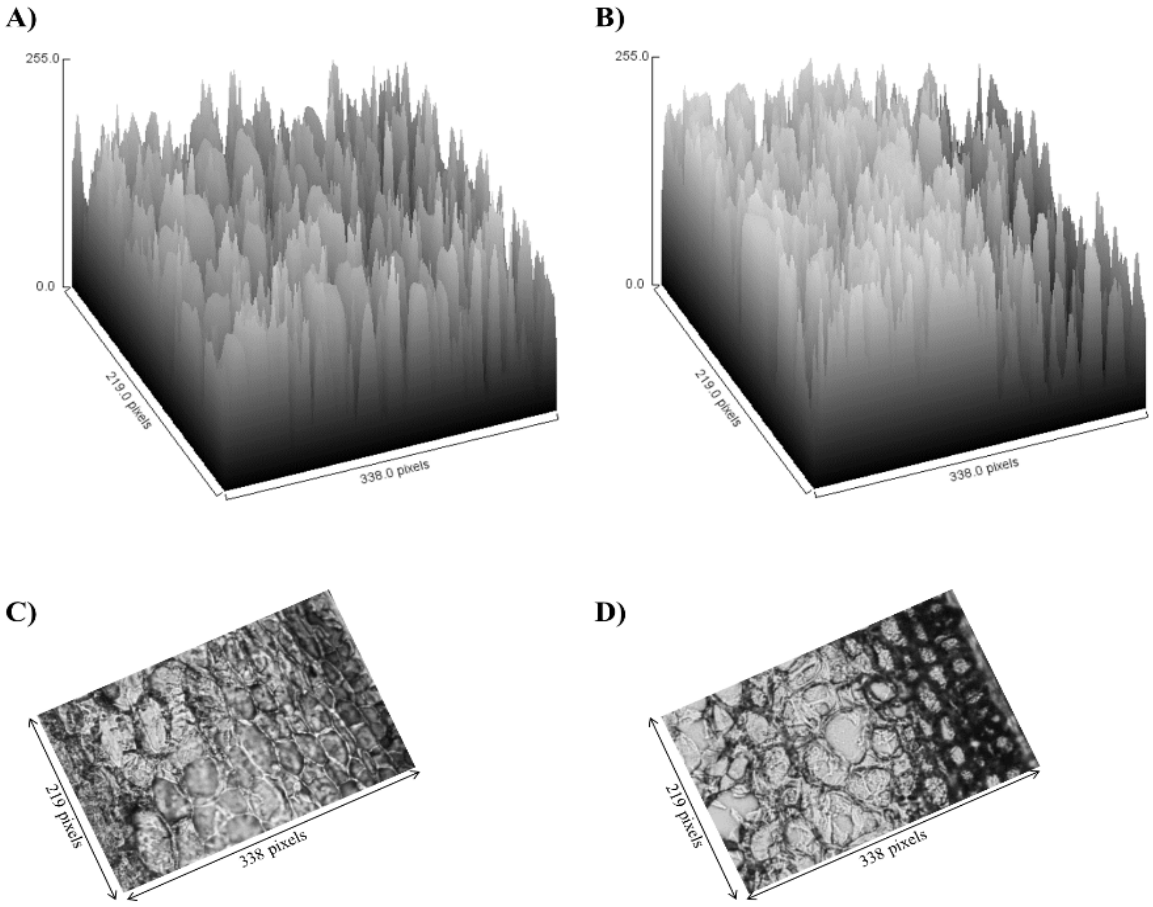

Figure 4. Examples of a surface plot of avocado pericarp tissue at A) Unripe stage and B) Ripe stage C) Unripe tissue image processed to obtain the surface plot. D) Ripe tissue image processed to obtain the surface plot.

3.5 Morphometric analysis per tissue section

Fractal dimension (F_D) values increased with the section for both ripening stages of avocado peel (Figure 5). This means that the exocarp of the avocado presented less heterogeneity in the cell arrangement in comparison to the inner of the tissue, which was more irregular. The ripening stage did not affect this tendency. However, an intersection point was observed in sections 4 and 5 between the two lines. In these sections, in unripe tissue, an increase in irregularity can be observed, which could be associated to the formation of idioblasts. Consequently, this point showed a change in trend in F_D values, which those for unripe avocado peel were significantly higher ($p < 0.05$) in comparison to the ripe tissue. On the other hand, lacunarity (Λ) values per tissue section presented the opposite trend that curves for F_D values for each ripening stage (Figure 6). A decrease in Λ values was observed in the analyzed tissue section and the ripening stage did not affect this trend. Sánchez-Segura *et al.* (2015) found also an inverse relation between F_D and Λ for tissues of pungent and non-pungent Capsicum species. The morphology of the epidermis of the avocado peel was less symmetric and gaps were not observed uniformly distributed in the entire image. In contrast, the inner tissue was more symmetric and uniform in irregularity. As well as F_D curves (Figure 5), an intersection point was observed in analyzed sections 4 and 5, which could explain a change in morphology in that location of the tissue, which corresponds to the parenchymal tissue with its lipid accumulation, giving evidence of a relation between F_D and Λ values.

A linear correlation was found between morphometric parameters (Λ and F_D) for each ripening stage (Figure 7) which indicated that the box

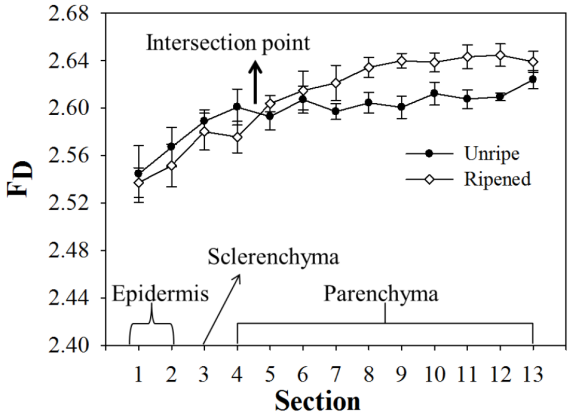

Figure 5. Fractal dimension (F_D) per tissue section at different ripening stages of avocado peel.?

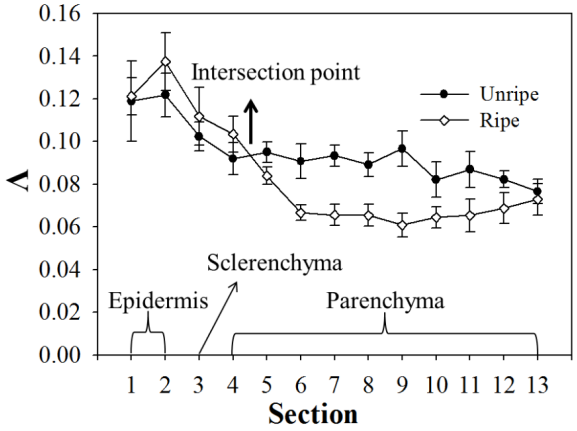

Figure 6. Lacunarity (Λ) per tissue section at different ripening stages of avocado peel.

was filled in the box-counting method with pixels in a similar manner that they were irregularly distributed in the entire image. Pearson's coefficient confirmed this correlation: -0.95 and -0.94 for unripe and ripe peel avocado, respectively. These negative Pearson's coefficients showed the inverse proportion between Λ and F_D which was explained above. According to the slope value for each ripening state, the F_D for unripe avocado tissue the change becomes pronounced in F_D than in Λ (higher value of slope), which explained a change in the filling of the gaps.

3.6 Confocal Laser Scanning Microscopy (CLSM)

The autofluorescence study showed the presence of two pigments distributed in the parenchymal and epidermal tissues, in immature avocado drymifolia fruit. The autofluorescence of chlorophyll was found at 673 nm emission in parenchymal tissue (Fig. 8A1). These observations confirmed the transition stages of maturity of parenchyma which cells came from the procambium (meristem tissue) which forms the vascular tissue of the fruit (Azcárraga-Rossette *et al.*, 2010). This tissue performs essential activities, such as photosynthesis, assimilation, respiration, storage, secretion, and excretion (Evert, 2006); in this case, accumulates chlorophylls (in chloroplasts) and lipids (in globules). The secondary autofluorescense signal was found between 472 nm to 683 nm and was attributed to lignin, localized in epidermis and hypodermis cells (Fig. 8A2). The merge image showed these signals came from isolated compounds in high concentrations (Fig. 8A3).

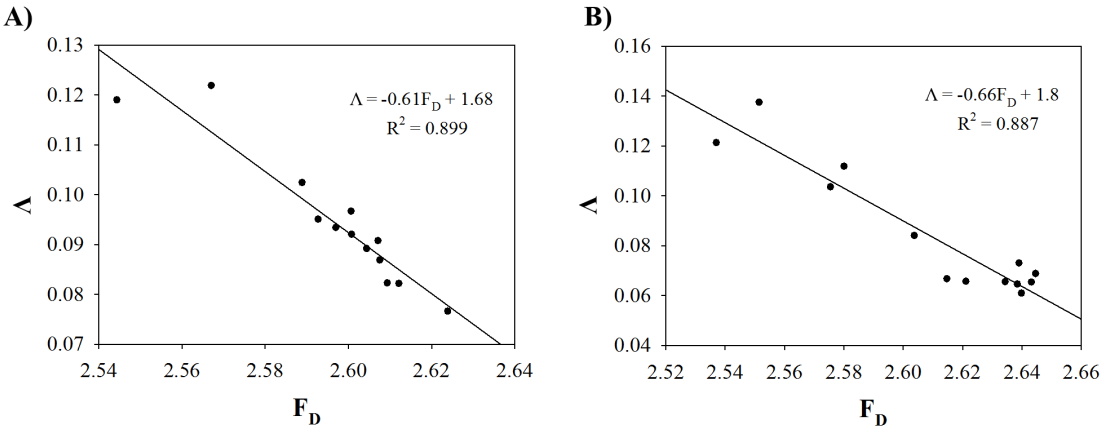

Figure 7. Correlation between lacunarity (λ) and fractal dimension (F_D) values with its corresponding linear equation regression and determination coefficient (R^2) for A) Unripe pericarp and for B) Ripe pericarp.

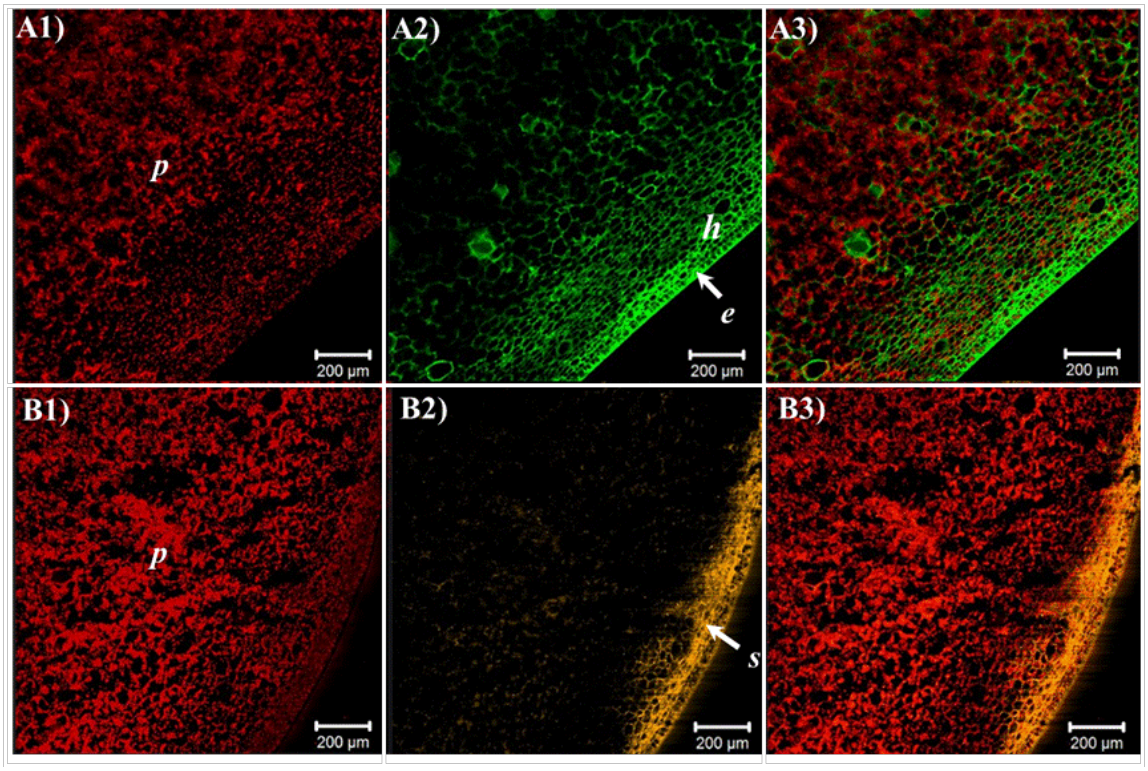

Figure 8. Autofluorescence signals for unripe and ripe avocado tissue obtained by means of CLSM. A1) In unripe avocado, the autofluorescence of chlorophyll was found in the parenchymal tissue (p). A2) and autofluorescense of lignin was localized in the epidermis (e) and in the hypodermis (h) tissues. A3) Merge image showed signal colocalization. B1) In ripe fruit, the chlorophylls autofluorescence is still observed in parenchymal tissue (p). B2) Anthocyanins compounds autofluorecence was observed in sclerenchymal tissue (s). B3) Merge image did not show colocalization of the signal.

In ripe avocado var. Drymifolia the autofluorescence of chlorophylls is also observed in parenchymal tissue (Fig. 8B1). However, we found that the autofluorescence signal of lignin was replaced by an anthocyanins signal, not because the lignin had disappeared in the tissue but because the anthocyanins concentration raised and had a stronger emission signal. The maximum peak excitation was found in sclerenchymal tissue at 645 nm, probably corresponding to anthocyanin compounds, presence already reported by other authors in Hass peel avocado (Ashton, 2006) (Fig. 8B2) Similar results were reported by Jin-Yuarn *et al*., 2008, they observed the range of excitation of pigments between 480 to 630 nm, which reflects a complex mixture of phenolic, flavonoids, and anthocyanins in red cabbage (*Brassica oleracea* L. var.). The merge image signals came from isolated compounds present in high concentration (Fig. 8B3).

Conclusions

Differences were found between unripe and ripe avocado var. drymifolia pericarp tissues. The Optical and Confocal Microscopy, fractal and lacunarity analysis, revealed significant differences between the two stages, demonstrating that during the ripening period important morphological changes take place. A more organized cell disposition, an increase in cell size and an important anthocyanin accumulation occurs during the ripening period. Brighter colors were observed for ripe peel avocado. The mode of the histogram plots for R, G and B channels was located towards higher values of pixel intensity.Fractal dimension (F_D) resulted higher for ripe tissues due to the irregular arrangement of cells whereas, F_D and lacunarity (Λ) analysis per tissue section demonstrated a morphology change in the section where lipid cell accumulation occurs.

Acknowledgments

The first author thanks CONACyT for financial support in the form of a study grant (275976). This study was supported by SIP projects 20150829 and 20160927.

References

Acosta-Díaz E., Hernández-Torres I., Almeyda-León I.H. (2012). Evaluación de aguacates criollos en Nuevo León, México: región sur. *Revista Mexicana de Ciencias Agrícolas 3*, 245-257.

Aguilera , J.M. (2001). Tamaño y forma de las partículas. En: *Métodos para Medir Propiedades Físicas en Industrias de Alimentos* (Alvarado JD. Ed.), Pp. 65-78 Acribia, España.

Arzate-Vázquez, I., Chanona-Pérez, J.J., Perea-Flores, M.J., Calderón-Domínguez, G., Moreno-Armendáriz, M.A., Calvo, H., Godoy-Calderón, S., Quevedo, R., Gutiérrez-López G., (2011). Image processing applied to classification of avocado variety Hass (*Persea americana* Mill.) during the ripening process. *Food Bioprocess Technologies 4*, 1307-1313.

Azcárraga-Rossette, M.R., Jácquez, R.M.P., Bonfil, C.A., Sandoval, Z.E. (2010). *Atlas de Anatomía Vegetal*. UNAM: Universidad Nacional Autónoma de México-Facultad de Estudios Superiores Cuautitlán, First ed., pp. 43-71.

Baish J.W., Jain R.K. (2000) Fractals and cancer. *Cancer Research 60*, 3683-3689.

Borys, P., Krasowska, M., Grzywna, J.Z., Djamgoz, B.A., Mycielska, E.M. (2008). Lacunarity as a novel measure of cancer cells behaviour. *Biosystems 94*, 276-281.

Bower, J.P. and Cutting, J.G. Avocado fruit development and ripening physiology. In: Janick (ed.) *Horticultural Reviews 10*, 229-271. Timber Press, Portland, OR.

Cerón-Montes, G.I., San Martin-Martínez, E., Yáñez-Fernández, J.; Quezada-Cruz, M., Castro-Muñoz, R. (2015). Preliminary purification of anthocyanins from blue corn by adsorption and electrophoresis. *Revista Mexicana de Ingeniería Química 14*, 99-108.

Colín-Orozco J., Chanona-Pérez J., Perea-Flores, M.D.J., Pedroza-Islas, R. (2014). Changes in large deformation properties during dough fermentation by Lactobacillus strains and their relationship with microstructure. *Revista Mexicana de Ingeniería Química 13*, 457-471.

Cummings K. and Schroeder C.A. (1942). Anatomy of the avocado fruit. *California Avocado Society 27*, 56-64.

Dreher, M. L., y Davenport, A.J. (2013). Hass avocado composition and potential health effects. *Critical Reviews of Food Science and Nutrition 53*, 738-750.

Dong, P. (2000). Test of a new lacunarity estimation method for image texture analysis. *International Journal of Remote Sensing 21*, 3369-3373.

Dürrenberger M.B., Handsdrin S., Conde-Petit B., Escher F. (2001). Visualization of Food Structure by Confocal Laser Scanning Microscopy (CLSM). *Lebens Wiss u Technology 34*, 11-17.

Evert, R.F., (2006). *Esau?s Plant Anatomy*. Meristems, Cells, and Tissues of the Plant Body: Their Structure, Function, and Development, third ed. John Wiley & Sons, Inc., Hoboken, New Jersey, pp. 447-466.

Fan-Chiang H.J., Wrolstad R.E. (2005) Anthocyanin pigment composition of blackberries. *Food Chemistry and Toxicology 70*, 198-202.

Fernández L., Castillero C., Aguilera, J. (2005). An application of image analysis to dehydration of apple discs. *Journal of Food Engineering 67*, 185-193.

Fisher B.J. and Davenport L.T. (1989). Structure and development of surface deformations on avocado fruits. *Horticultural Science 24*, 841-844.

García-Armenta E. (2015). *Estudio morfométrico del patrón de ruptura de alimentos*. Tesis doctoral. Programa de Doctorado en Alimentos. Instituto Politécnico Nacional.

García-Armenta E., Téllez-Medina D.I., Alamilla-Beltrán L., Arana-Errasquín R., Hernández-Sánchez H., Gutiérrez-López G.F. (2014) Multifractal breakage patterns of thick

maltodextrin agglomerates. *Powder Technology 266*, 440-446.

García-Armenta E., Téllez-Medina D.I., Sánchez-Segura L., Alamilla-Beltrán L., Hernández-Sánchez H., Gutiérrez-López G.F. (2016). Multifractal breakage pattern of tortilla chips as related to moisture content. *Journal of Food Engineering 168*, 96-104.

Giovannoni J. (2011). Molecular biology of fruit maturation and ripening. *Annual Review of Plant Physiology and Plant Molecular Biology 52*, 725-749.

Jin-Yuarn L., Chia-Yuan L., I-Farn H. (2008). Characterisation of the pigment components in red cabbage (*Brassica oleracea* L. var.) juice and their anti-inflammatory effects on LPS-stimulated murinesplenocytes. *Food Chemistry 109*, 771-781.

Kilic, I.,K., Abiyev, H., H., R., (2011). Exploiting the synergy between fractal dimension and lacunarity for improved texture recognition. *Signal Process 91*, 2332-2344.

Kodagali, A.J., Balaji, S.(2012) Computer vision and image analysis based techniques for automatic characterization of fruits-a review. *International Journal Computer Applications 50*, 0975-8887.

Kosinska, A., Karamac, M., Estrella, I., Hernández, T., Bartolomé, B., Dykes, G.A. (2012) Phenolic compounds profiles and antioxidant capacity of *Persea americana* Mill. Peels and seeds of two varieties. *Journal of Agricultural Food Chemistry 60*, 4613-4619.

León, K., Mery D., Pedreschi F., León J. (2006). Color measurement in L* a* b* units from RGB digital images. *Food Research International 39*,1084-1091.

Lila M.A. (2004) Anthocyanins and human health: an in vitro investigative approach. *Journal of Biomedicine and Biotechnology 5*, 306-13.

Luza J.G., Lizana L.A. (1992) Ultrastructure and Cytology of the Postharvest Avocado (*Persea americana* Mill). *Proceedings of Second World Avocado Congress*, 443-448.

Mandelbrot, B.B. (1983). *The Fractal Geometry of Nature*. WH Freeman and Co New York, USA.

Mendoza F., Dejmeck P., Aguilera J.M. (2006). Calibrated color measurement of agricultural foods using image analysis. *Postharvest Biology and Technology 4*, 285-295

Paddock S.W. (1999). Confocal Laser Scanning Microscopy. *Biotechniques 27*, 992.

Platt-Aloia K.A., Thomson W.W. (1992). Ultrastructure of avocados: ripening, chilling injury, and isolation of idioblast oil cells. *Proceedings of the Second World Avocado Congress*, 417-425.

Plotnick, R.E., Gardner, R.H., Hargrove, W.W., Prestegaard, K., Perlmutter, M. (1996). Lacunarity analysis: a general technique for the analysis of spatial patterns. *Physical Reviews 53*, 5461.

Quevedo, R., Mendoza, F., Aguilera, J.M.,Chanona, J., Gutiérrez-López, G.(2008). Determination of senescent spotting in banana (*Musa Cavendish*) using fractal texture Fourier image. *Journal of Food Engineering 84*, 509-515.

Sánchez-Segura L., Téllez-Medina D.I., Evangelista-Lozano S., García-Armenta E., Alamilla-Beltrán L., Hernández-Sánchez H., Jiménez-Aparicio A.R., Gutiérrez-López G.F. (2015)Morpho-structural description of epidermal tissues related to pungency of *Capsicum* species. *Journal of Food Engineering 152*, 95-104.

Santacruz-Vázquez C., Santacruz-Vázquez V., Chanona-Pérez J., Jaramillo-Flores MA., Welti-Chanes J., Gutiérrez-López G.(2007) Fractal Theory Applied to Food Science. *Encyclopedia of Agricultural, Food, and Biological Engineering 1*, 1-13.

Schroeder A.C. (1953). Growth and development of the *fuerte* avocado fruit. *Proceedings of the Society for Horticultural Science 6*, 103-109.

Schroeder A.C. (1950). The structure of the skin or rind of the avocado. *California Avocado Society 1950 Yearbook 34*, 169-176.

SIAP (Sistema de Información Agrícola y Pesquera) Información de producción del aguacate criollo durante el cierre del año 2014. Available in: http://www.siap.gob.mx/cierre-de-la-produccion-agricola-por-cultivo.

Stach, S. y Cybo, J. (2003). Multifractal description of fracture morphology: theoretical bases. *Materials Characterization 51*, 79-86.

Stintzing F.C., Carle R.(2004) Functional properties of anthocyanins and betalains in plants, food and in human nutrition. *Trends in Food Science & Technology 15*, 19-38.

Wang, W., Bostic, T.R., Gu, L. (2010). Antioxidant capacities, procyanidins and pigments in avocados of different strains and cultivars. *Journal of Food Chemistry 122*, 1193-1198.

Yam K.L., Papadakis S.E. (2004). A simple digital imaging method for measuring and analyzing color of food surfaces. *Journal of Food Engineering 61*, 137-142.